

Investigation of electronic structure of the alloys Nb₃Al and Nb₃Sn by the thermoreflection method

A. I. Golovashkin, I. S. Levchenko, and A. L. Shelekhov

P. N. Lebedev Physics Institute, USSR Academy of Sciences

(Submitted 29 November 1983)

Zh. Eksp. Teor. Fiz. **86**, 2229–2238 (June 1984)

The thermoreflection spectra of Nb₃Sn and of Nb–Al alloys were measured in the 0.5–0.3 range. An algorithm is proposed for the density of the electron states on the basis of the form of the thermomodulation spectra of two-phase samples. A number of electronic characteristics of Nb₃Sn and Nb₃Al are determined, as well as their temperature dependence coefficients. Splitting of the interband absorption band located in the 1.85-eV region is observed. The splitting is apparently due to the influence of the hybridization of the *d* and *s* states of the alloy. The density of the electron states $N(E_F)$ near the Fermi energy is estimated. The decrease of the value of $N(E_F)$ for the Nb₃Al alloy with decreasing mean free path of the electrons is attributed to the smearing of the sharp singularity in the density of the electron states near E_F .

INTRODUCTION

The properties of alloys with A15 lattice are being diligently investigated of late both theoretically and experimentally. The reason is that some compounds of this type have superconductivity with high critical parameters. The study of such superconductors is a step towards the attainment of high superconducting temperatures. However, whereas the theoretical studies are devoted to the band structure of this class of compounds, the experiments deal mainly with their superconducting properties and only a few experiments are devoted to a determination of the characteristic of the electronic structure. Experimental research into the electronic structure of A15-lattice alloys is of great interest both for superconductivity and for solid-state physics in general. Thus, for example, a number of theoretical studies^{1–8} point to the possibility that such compounds having sharp peaks in the density of the electronic states. The high critical temperatures of superconductors with A15 lattice are attributed to the location of the Fermi level near the maximum of one such peak. The validity of this statement can be verified experimentally by investigating the electronic structure of such compounds.

Valuable information on the electronic structure of a metal or alloy can be obtained by the method of optic thermomodulation spectra (TMS). This method is successfully used at present in investigations of the electronic structure of both simple and transition metals and their alloys.^{9–13} Using a theoretical model of the TMS,¹⁴ based on Bragg interband transitions, it is possible to obtain from the thermoreflection spectra an extensive set of very important electronic characteristics of the investigated material, viz., the Fourier component V_g of the pseudopotential with index “*g*,” the effective densities and collision frequencies N_g and ν_g of the electrons that participate in the interband transitions near the Bragg planes {*g*}, the density N_e and frequency ν_e of the conduction electrons, as well as the corresponding coefficients K_N , K_V and K_ν of the temperature dependences of N_e , V_g , and the collision frequencies, respectively.

We have measured the thermostimulation reflection

spectra $\beta(\omega) = d(\ln R)/dT$, where R is the light-reflection coefficient and T is the temperature of the Nb₃Sn sample and of two Nb–Al alloy samples. From the experimental β spectra we determined a number of electronic characteristics of the alloys Nb₃Sn and Nb₃Al.

DETAILS OF EXPERIMENT

The alloy samples investigated were polycrystalline films deposited by the electron-beam method¹⁵ in a vacuum $\approx 10^{-6}$ Torr on heated sapphire substrates. The characteristics of the samples are listed in Table I, where T_c is the superconducting-transition temperature, d is the plasma thickness, R_r/R_{res} is the ratio of the resistances at room temperature and a temperature somewhat higher than T_c , and a is the lattice constant.

An x-ray analysis of the Nb₃Sn sample has shown it to contain only the A15 phase. The Nb–Al sample No. 1 is inhomogeneous, but its A15 content is not less than 80%. Although the superconducting transition temperature of Nb–Al sample No. 2 is higher than that of No. 1, its A15 content is lower.

The thermomodulation reflection spectra were measured at room temperatures in the spectral range 0.5–3.2 eV with a previously described setup.¹⁶ In the course of the experiment the temperature of the investigated sample was modulated at a frequency 23 Hz by a pulsed current. The depth of temperature modulation was 0.6–2 K for the different samples. Repeated accumulation of the signal in the memory of the multichannel analyzer (each spectrum was recorded several hundred times) has made it possible to obtain experimental curves accurate to $\sim 2 \times 10^{-6}$ deg⁻¹. The

TABLE I. Characteristics of samples.

| sample | T_c , K | d , μm | R_r/R_{res} | a , \AA |
|--------------------|-----------|---------------------|---------------|--------------------|
| Nb ₃ Sn | 17.6 | 0.35 | 2.7 | 5.22 |
| Nb – Al № 1 | 16.0 | 0.2 | 2.55 | 5.19 |
| Nb – Al № 2 | 16.5 | 0.25 | 2.2 | – |

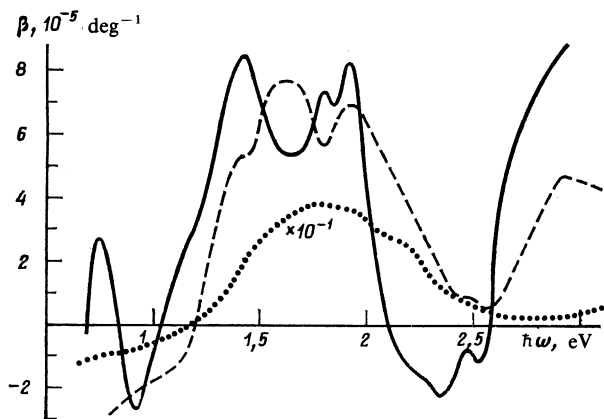


FIG. 1. Experimental TMS of Nb_3Sn (solid curve), Nb-Al No. 1 (dashed), and Nb-Al No. 2 (dotted).

information obtained from the experiment was fed to a computer, where the data were reduced further.

RESULTS

The experimental TMS of Nb_3Sn and of the two Nb-Al spectra are shown in Fig. 1. The Nb_3Sn spectrum shows four pronounced absorption bands with maxima at 0.75, 1.43, 1.85, and 2.95 eV. Besides the main bands, the TMS of Nb_3Sn shows a fine structure. The TMS of the first Nb-Al sample also contains four main absorption bands with maxima at 1.4, 1.6, 2, and 3 eV. The character of the spectrum in the long-wave region points to the presence of a fifth absorption band at energy $\hbar\omega < 1$ eV. The TMS of the Nb_3Sn and of the first Nb-Al sample are close in intensity and similar in structure, except for the band in the 1.6 eV region. This band, in our opinion, is due to the presence in the Nb-Al phase of niobium, which has at $\hbar\omega \approx 1.6$ eV a strong interband absorption band.¹⁷ The spectrum of the second Nb-Al sample is more diffuse and its intensity is several times higher than the TMS of Nb_3Sn and of the first Nb-Al sample. The principal maximum of the spectrum is located in the region 1.5–2 eV, and the interband absorption spectra manifest themselves only in the form of singularities. This is evidence of the poorer quality of the second sample, in which the electron mean free path is shorter.

Assuming that the absorption bands observed on the TMS are Bragg electronic interband transitions, the experimental TMS were reduced with a computer, using the algorithm and the programs of Refs. 14 and 18. In the reduction, the experimental TMS was approximated, using least squares, by a theoretical β spectrum based on the model of Bragg interband electronic transitions.¹⁹

Since the investigated samples can contain in many cases other phases (this pertains in particular to metastable high-temperature superconductors with A15 lattice), the influence of the foreign phases on the TMS was taken into account by modifying somewhat the calculation formulas of Ref. 14.

In the case when the sample consists of two phases uniformly and randomly distributed, with the sizes of the individual phase regions large enough (to be able to neglect interface effects), $\beta(\omega)$ can be expressed in the form

$$\beta(\omega) = \frac{1}{R} \frac{dR}{dT} \approx \frac{1}{\Delta T} \frac{\Delta R_1 + s \Delta R_2}{R_1 + s R_2}, \quad (1)$$

where R is the "effective" coefficient of light reflection from the sample, R_1 and R_2 are respectively the coefficients of light reflection from the first and second phases of the sample, $s = s_2/s_1$ is the relative sample surface area occupied by the second phase (s_1 and s_2 are respectively the areas of the first and second phases). For a uniform distribution of the phases the value of s coincides with the relative bulk concentration of the second phase (as well as with the weight concentration if the phase densities are close), while s_1 and s_2 can be regarded in our case as the bulk concentrations of the first and second phases. The quantities ΔR_1 and ΔR_2 characterize the changes of the light reflection coefficient following a temperature change ΔT .

Knowing the electronic characteristics of one of the phases, which determine its optical properties, it is possible to obtain from the experimental spectrum of the two-phase sample not only the electronic characteristics of the second phase, but also the parameter s in terms of which the concentrations of the two phases are readily determined: $s_1 = (1 + s)^{-1}$, $s_2 = s(1 + s)^{-1}$. The relations obtained were used in the reduction of the TMS of the two-phase Nb-Al samples as well as the one-phase Nb_3Sn sample, with niobium assuming the role of the second phase.

The electronic characteristics of Nb_3Sn and Nb_3Al obtained by reduction of the TMS of various samples are given in Table II. The table lists also the values obtained for the density $N(E_F)$ of the electronic states near the Fermi surface. The values of $N(E_F)$ were calculated from the formula of Ref. 13. In the calculation we used the values of the average electron velocity v_F on the Fermi surface, given in Table II and obtained by linear interpolation from the v_F of Refs. 3 and 7 and from the free-electron velocity on the Fermi sphere at a density N_e equal to that of the valence electrons. By v_F is meant here $\langle v_F^2 \rangle^{1/2}$.

The calculation errors do not exceed several per cent for the basic electronic characteristics, 5–15% for N_g , and 20–

TABLE II. Electronic characteristics of Nb_3Sn and Nb_3Al .

| Characteristic | Nb_3Sn | Nb_3Al (№ 1) | Nb_3Al (№ 2) |
|-----------------------------------------------------|------------------------|------------------------------|------------------------------|
| V_{200} , eV | 1.37 | 1.35 | 0.93 |
| V_{210} , eV | 0.56 | 0.6 | 0.47 |
| V_{211} , eV | 0.35 | 0.26 | 0.22 |
| V_{310} , eV | 0.92 | 0.93 | 0.74 |
| v_{200} , 10^{14} , sec^{-1} | 9 | 4.2 | 5.1 |
| v_{210} , 10^{14} , sec^{-1} | 9 | 1.3 | 6.0 |
| v_{211} , 10^{14} , sec^{-1} | 2 | 1 | 2.4 |
| v_{310} , 10^{14} , sec^{-1} | 3 | 2.6 | 5.8 |
| N_{200} , 10^{22} , cm^{-3} | 0.09 | 0.03 | 0.25 |
| N_{210} , 10^{22} , cm^{-3} | 0.25 | 0.06 | 0.69 |
| N_{211} , 10^{22} , cm^{-3} | 0.17 | 0.04 | 0.4 |
| N_{310} , 10^{22} , cm^{-3} | 0.03 | 0.06 | 0.37 |
| N_e , 10^{22} , cm^{-3} | 1.6 | 2.4 | 4.2 |
| v_F , 10^{14} , sec^{-1} | 1.5 | 1.0 | 2.9 |
| K_M , 10^{-4} , deg^{-1} | 7 | 4 | 5 |
| K_V , 10^{-4} , deg^{-1} | -0.4 | -2 | -40 |
| K_{ω} , 10^{-3} , deg^{-1} | 4 | 1 | 8 |
| s_1 , % | 100 | 72 | 33 |
| v_F , 10^8 cm/sec | 0.4 | 0.4 | 0.6 |
| $N(E_F)$, $\frac{\text{state}}{\text{eV-at-spin}}$ | 0.44 | 0.65 | 0.5 |
| l , Å | 30 | 40 | 20 |

40% for the temperature coefficients; s_1 is accurate to 3–4%. The inaccuracy of the determination of the electronic characteristics of the useful phase decreases with increasing concentration of the latter in the sample; the inaccuracy of the theoretical model is $\sim V_g/E_F$.

It can be seen from Table II that the percentages of the A15 phase in the Nb_3Sn and Nb-Al samples, calculated from the TMS, are in full agreement with the results of the x-ray analysis.

To verify the capabilities of the procedure we measured and reduced the TMS of a third Nb-Al sample containing even less of the A15 phase than sample No. 2. The TMS of sample No. 3 is close in intensity and in general shape to the β spectrum of the second sample, but it does not have even those singularities that can be seen on the β spectrum of sample No. 2. The A15-phase content in this sample was shown by the TMS reduction to be less than 10%. We did not succeed in determining with sufficient reliability the electronic characteristics of the A15 phase of this sample.

The Nb_3Sn thermomodulation spectrum calculated on the basis of the electronic characteristics of Table II is compared in Fig. 2 with the experimental TMS. The figure reveals a good enough agreement of the two spectra, both in shape and in intensity of the bands. The theoretical model does not describe the spectrum fine structure observed in experiment for sufficiently good samples.

The form of the Nb_3Al β spectra calculated on the basis of the data obtained is shown in Fig. 3. In analogy with the results observed for Nb (Ref. 13), the TMS of the more finely dispersed sample is more strongly smeared out and is considerably more intense. Its main absorption bands are shifted into the long-wave region of the spectrum.

The electronic characteristics obtained by analyzing the TMS permit calculation of the spectral dependences of the optical constants. Figures 4 and 5 show the obtained spectra of the optical conductivity of the Nb_3Sn and Nb_3Al . For Nb_3Al we used the data of the first sample. The dash-dot curve shows the contribution of the conduction electrons, the dashed the contribution of the interband electronic transitions, and the dotted the contributions of the individual bands. The alloy Nb_3Sn was investigated in Refs. 20 by the

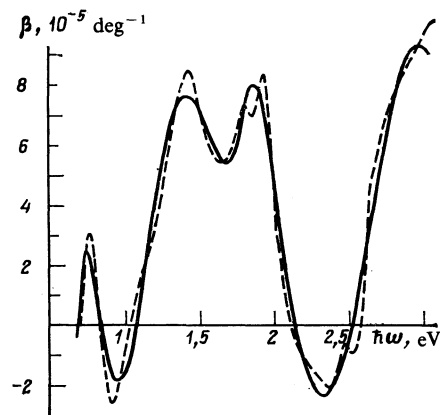


FIG. 2. Experimental (dashed curve) and theoretical (solid) β spectra of Nb_3Sn .

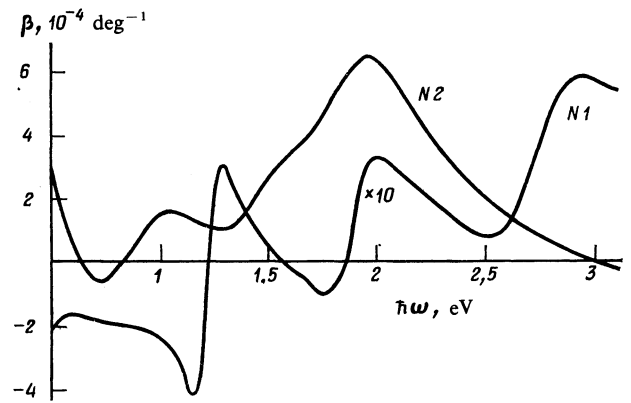


FIG. 3. TMS of Nb_3Al calculated on the basis of the data of Table II.

polarization optics method. The electronic characteristics of Nb_3Sn listed in Table II are in good agreement with the data of Refs. 20, except for the parameters of the $\{310\}$ band.

Ellipsometric measurements of the optical properties of Nb-Al samples were made in Refs. 21 and 22. A direct comparison of our present results with the data of these references is difficult, since no account was taken in the latter of the presence of other phases in the samples. It can be noted, however, that in Refs. 21 and 22 there is observed in the 0.5–3 eV region a complicated structure of the spectra, which consist of a large number of interband-transition bands.

DISCUSSION

1. The method proposed in the present paper for determining the electronic characteristics of two-phase samples yielded quite reasonable results. For the one-phase Nb_3Sn sample it was found from the TMS, accurate to several per cent, that the concentration of the A15 phase is 100%. The electronic characteristics of the sample agree with those obtained using the algorithm of Ref. 14.

In the calculations of the electronic characteristics of Nb_3Sn and Nb_3Al we used for Nb the data of Ref. 17. It is

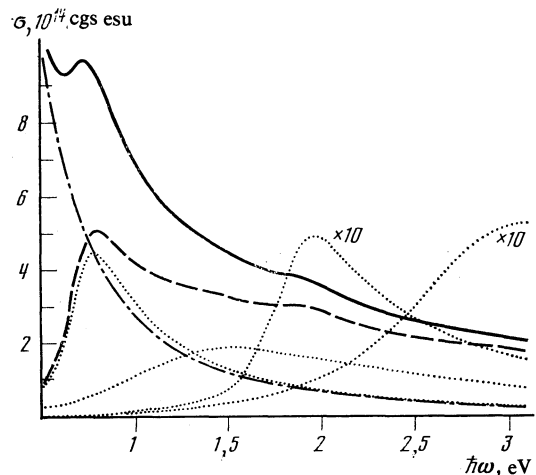


FIG. 4. Spectrum of the optical conductivity $\sigma(\omega)$ of Nb_3Sn (solid curve), contribution to $\sigma(\omega)$ from the conduction electrons (dash-dot) and from the Bragg interband electronic transitions (dashed curve), and contribution to $\sigma(\omega)$ from the individual interband-absorption bands (dotted).

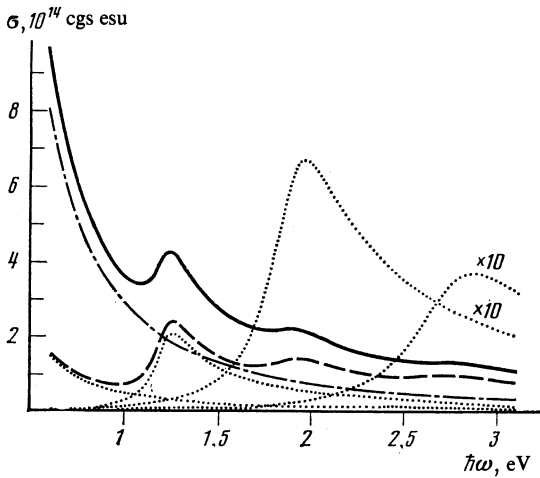


FIG. 5. Spectrum of optical conductivity of Nb₃Al (solid curve), contribution to $\sigma(\omega)$ from the conduction electrons (dash-dot) and from the Bragg interband transitions (dashed), and contribution to $\sigma(\omega)$ from the individual interband-absorption bands (dotted).

known¹³ that the characteristics of Nb depend somewhat on the sample quality.

A criterion of the validity of the data used for Nb is the agreement of the coefficient s_1 with the value obtained by an independent method. We note that at high concentration of the investigated phase some variation of the Nb parameters hardly alters the obtained basic characteristics. At a low content of the phase (Nb–Al sample No. 2) the effect of the inaccuracy of the Nb parameters is already appreciable, but the results for this sample are only approximate.

2. The observed deterioration of the TMS of Nb₃Al samples of poorer quality (disorder, decrease of electron mean free path in the sample) is in full accord with the results obtained for niobium.¹³ Just as in Nb, an increased smearing of the energy gaps, an increase of the conduction-electron density, and a shortening of the electron relaxation time are observed. The temperature dependence of a number of characteristics increases in this case (it is this which leads to the higher intensity of the β spectrum). Thus, the results of Nb₃Al confirm the conclusions of Ref. 13 that the electronic characteristics and the optical properties are influenced by the smearing of the sharp singularities of the density of the electronic states.

3. Our values of the plasma frequencies ω_p correspond to $\hbar\omega_p = 4.7$ and 5.8 for Nb₃Sn and Nb₃Al, respectively. The published data, 3.4 eV (Ref. 3) and 4.5 eV (Ref. 23) for Nb₃Sn and 3.7 eV for Nb₃Al (Ref. 7) are somewhat lower than ours. We attribute this difference to the shorter electron mean free

paths in our samples, which lead to larger values of N_e (Ref. 13). It must be noted that within the framework of the model employed the interband transitions displace the point at which the real part of the dielectric constant vanishes towards high values of ω (compared with ω_p).

4. The most important characteristic of high-temperature superconductors, $N(E_F)$, was determined for Nb₃Sn and Nb₃Al both experimentally and theoretically in a large number studies. In Table III our data are compared with the published ones (the data on Nb₃Al are given only for sample No. 1). It is seen from the table our values of $N(E_F)$ do not go outside the scatter of the data. In Nb₃Al sample No. 2 the density of states is noticeably smaller than in the first, and this is evidence of the smearing of the $N(E_F)$ peak in Nb₃Al when the electron mean free path l is decreased from 40 to 20 Å.

5. The thermomodulation spectrum of a metal or an alloy is determined by the temperature dependence of the light-reflection coefficient. This dependence is in turn a consequence of the temperature dependences of the real (ε_1) and imaginary (ε_2) parts of the complex dielectric constant. To determine the contributions of ε_1 and ε_2 to the TMS we can represent $\beta(\omega)$ in the form

$$\beta(\omega) = \frac{\Delta R}{R} \frac{1}{\Delta T} = \frac{1}{\Delta T} \{a(\varepsilon_1; \varepsilon_2) \Delta \varepsilon_1 + b(\varepsilon_1; \varepsilon_2) \Delta \varepsilon_2\}, \quad (2)$$

where $\Delta \varepsilon_1$ and $\Delta \varepsilon_2$ are respectively the changes of ε_1 and ε_2 following a temperature change ΔT . The quantities $a(\varepsilon_1; \varepsilon_2)$ and $b(\varepsilon_1; \varepsilon_2)$ are determined by the relations

$$a(\varepsilon_1; \varepsilon_2) = \frac{\sqrt{2}(\varepsilon + \varepsilon_1)(2\varepsilon_1 - \varepsilon - 1)}{\varepsilon(\varepsilon + \varepsilon_1)^{3/2}((1 + \varepsilon)^2 - 2(\varepsilon + \varepsilon_1))}$$

$$b(\varepsilon_1; \varepsilon_2) = \frac{\sqrt{2}\varepsilon_2(2\varepsilon_1 + \varepsilon - 1)}{\varepsilon(\varepsilon + \varepsilon_1)^{3/2}((1 + \varepsilon)^2 - 2(\varepsilon + \varepsilon_1))},$$

where $\varepsilon = (\varepsilon_1^2 + \varepsilon_2^2)^{1/2}$.

Figure 6 shows the spectral dependences of $\Delta \varepsilon_1$ and $\Delta \varepsilon_2$ for Nb₃Sn (a) and Nb₃Al (b), calculated on the basis of the obtained electronic characteristics. As seen from the figures, the singularities due to interband transitions are more pronounced in the $\Delta \varepsilon_2$ spectrum. The quantities $a(\varepsilon_1; \varepsilon_2)$ and $b(\varepsilon_1; \varepsilon_2)$ are monotonic functions of the frequency ω . An analysis of Eq. (2) has shown that the basic structure of the TMS of both alloys is determined by the contribution from the temperature dependence of ε_2 [the second term of (2)].

6. The experimental TMS of Nb₃Sn shows a clear-cut splitting of the interband-absorption band in the region of 1.85 eV; the splitting amounts to 0.125 eV. This splitting can

TABLE III. Density of electronic state at the Fermi energy in Nb₃Sn and Nb₃Al.

| $N(E_F)$, $\frac{\text{state}}{\text{eV}\cdot\text{at}\cdot\text{spin}}$ | | Source | $N(E_F)$, $\frac{\text{states}}{\text{eV}\cdot\text{at}\cdot\text{spin}}$ | | Source |
|---------------------------------------------------------------------------|--------------------|--------------------|----------------------------------------------------------------------------|--------------------|--------------|
| Nb ₃ Sn | Nb ₃ Al | | Nb ₃ Sn | Nb ₃ Al | |
| — | 0.83 | [24] | 0.46 | 0.37 | [6] |
| 0.45 | 0.52 | [2] | — | 0.9 | [7] |
| 1.12 | 0.82 | Junod (see Ref. 2) | — | 0.97 | [5] |
| 1.2 | 0.8 | | [25] | 0.92 | — |
| 0.44 | — | [3] | 0.44 | 0.65 | Present work |

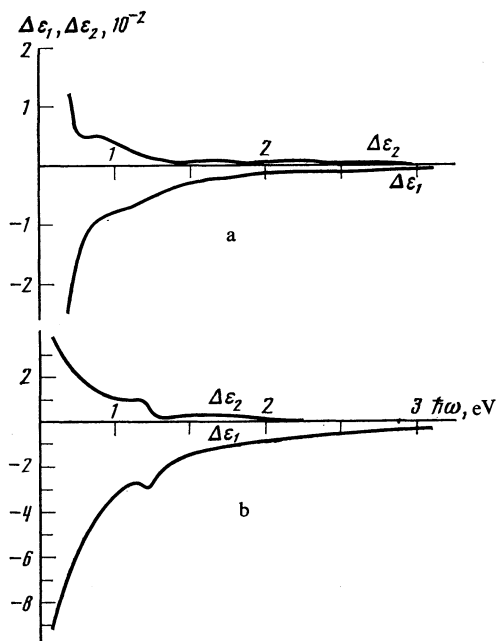


FIG. 6. Spectral dependences of $\Delta \varepsilon_1$ and $\Delta \varepsilon_2$ for the alloys Nb_3Sn (a) and Nb_3Al (b).

be due to the energy-band splitting by the hybridization of the s - p and d states near the Bragg plane, and to formation of corresponding energy subbands.²⁷ The initial d band can be located in this case either below or above E_g . The interband-absorption band due to the electronic interband transitions near this plane is split into two, with the higher-frequency band the result of excitation of electrons from or to d levels, and the lower-frequency one caused by transitions between s - p levels.

Since an appreciable contribution is made to the intensity of the bands in the β spectrum by the temperature dependence of the electron relaxation times (i.e., of the values of ν_g), one should expect a comparable intensity for both parts of the split band, since each of the transition affects the s - p states. It is this which is observed on the TMS of Nb_3Sn for the band in the 1.85 eV region. Our theoretical model of the TMS does not take the indicated band splitting into account. According to the foregoing interpretation of the observed splitting, the values of V_g and ν_g given in Table II for transitions near $\{310\}$ planes are somewhat overevaluated, but we estimate the error not to exceed 6%.

For Nb_3Al no splitting of the $\{310\}$ band is observed, although in all other respects the spectra of Nb_3Sn and Nb_3Al are similar. This can be due to the smaller splitting of the band in Nb_3Al and to the smearing of its fine structure. This explanation can also be indicated by the fact that even in the best Nb_3Al sample the $\{310\}$ band is broader than the corresponding band in Nb_3Sn , although the electron mean free path in Nb_3Al is longer.

The errors of V_g and ν_g of Nb_3Al , due to the influence of the interband transitions from or two d -type levels, are smaller than for Nb_3Sn . The singularities observed on the TMS of Nb_3Sn and of the first Nb-Al sample in the region of 2.5 eV are also apparently due to the influence exerted on the

spectrum by transitions, connected with the d states, in other regions of phase space.

7. Reviewing the data obtained for V_g and ν_g in the present study, several features can be noted. For both alloys we have $\hbar\nu_g < 2V_g$, so that the level smearing, represented by the quantity $\hbar\nu_g$, does not distort substantially the structure of the energy gaps near the Bragg planes. The value of ν_g of Nb_3Al sample No. 1 increases monotonically with V_g , and it can be said that Nb_3Sn and sample No. 2 of Nb_3Al have a similar tendency (just as Nb in Ref. 13). Next, $\nu_g \gtrsim \nu_e$ for all bands of both alloys. Explanation of all these facts calls for an examination of the details of the mechanism electron relaxation in the presence of a Bragg energy splitting.

The authors thank N. N. Lobanov for the x-ray analysis of the samples and T. I. Kuznetsova for a discussion of the results.

¹M. Weger, *Rev. Mod. Phys.* **36**, 175 (1964).

²L. F. Mattheiss, *Phys. Rev.* **B12**, 2161 (1975).

³L. F. Mattheiss, L. R. Testardi, and W. W. Yao, *Phys. Rev.* **B17**, 4640 (1978).

⁴L. Testardi, M. Weger, and I. Goldberg, *Russ. transl. in: Superconducting Compounds with β -Tungsten Structure*, Mir, 1977, p. 435.

⁵W. E. Pickett, K. M. Ho, and M. L. Cohen, *Phys. Rev.* **B19**, 1734 (1979).

⁶G. Arbman, *Sol. State Commun.* **26**, 857 (1978).

⁷P. B. Allen, W. E. Pickett, K. M. Ho *et al.*; *Phys. Rev. Lett.* **40**, 1532 (1978).

⁸R. N. Blatt, *Phys. Rev.* **B16**, 1915 (1977).

⁹A. I. Golovashkin, K. V. Mitsek, and G. P. Motulevich, *Fiz. Tverd. Tela (Leningrad)* **14**, 1704 (1972) [*Sov. Phys. Solid State* **14**, 1467 (1972)].

¹⁰A. I. Golovashkin, D. R. Dzhurav, I. S. Levchenko *et al.*, *ibid.* **19**, 2427 (1977) [**22**, 1420 (1977)].

¹¹J. H. Weaver, D. W. Lynch, C. H. Culp *et al.*, *Phys. Rev.* **B14**, 459 (1976).

¹²G. A. Fraser and R. Glosser, *Sol. State Commun.* **41**, 245 (1982).

¹³A. I. Golovashkin and A. L. Shelekhov, *Zh. Eksp. Teor. Fiz.* **84**, 2141 (1983) [*Sov. Phys.* **57**, 1246 (1983)].

¹⁴A. I. Golovashkin and A. L. Shelekhov, *Kr. soobshch. fiz.* No. 5, 11 (1978); *FIAN Preprint No. 96*, 1981.

¹⁵A. I. Golovashkin, I. S. Levchenko, and G. P. Motulevich, *Trudy FIAN* **82**, 72 (1975).

¹⁶A. I. Golovashkin and A. L. Shelekhov, *Prib. Tekh. Eksp.* No. 5, 216 (1980); *FIAN Preprint No. 71*, 1979.

¹⁷A. I. Golovashkin and A. L. Shelekhov, *Fiz. Tverd. Tela (Leningrad)* **24**, 3339 (1982) [*Sov. Phys. Solid State* **24**, 1897 (1982)].

¹⁸A. I. Golovashkin and A. L. Shelekhov, *FIAN Preprint No. 134*, 1981.

¹⁹A. I. Golovashkin and G. P. Motulevich, *Zh. Eksp. Teor. Fiz.* **57**, 1054 (1969) [*Sov. Phys. JETP* **30**, 575 (1970)]; *FIAN Preprint No. 76*, 1969.

²⁰A. I. Golovashkin and G. P. Motulevich, *Usp. Fiz. Nauk* **111**, 554 (1973) [*Sov. Phys. Usp.* **16**, 940 (1974)]; G. P. Motulevich, A. I. Golovashkin, and A. A. Shubin, in: *Elektronnaya struktura perekhodnykh metallov, ikh splavov i soedinenii* (Electronic Structure of Transition Metals, Their Alloys, and Compounds), Kiev, Naukova dumka, 1974, p. 311.

²¹N. D. Kuz'michev, I. S. Levchenko, and G. P. Motulevich, *FIAN Preprint No. 27*, 1983.

²²L. T. Burkova and I. S. Levchenko, *Kratk. soobshch. fiz.* No. 1, 40 (1979).

²³I. Tutto, L. M. Kahn, and J. Ruvalds, *Phys. Rev.* **B20**, 952 (1979).

²⁴R. H. Willens, T. H. Geballe, A. C. Gossard, J. P. Maita *et al.*, *Sol. State Commun.* **7**, 837 (1969).

²⁵G. S. Knapp, S. D. Bader, and Z. Fisk, *Phys. Rev.* **B13**, 783 (1976).

²⁶T. P. Orlando, E. J. McNiff, S. Foner, and M. R. Beasley, *Phys. Rev.* **B19**, 4545 (1979).

²⁷A. I. Golovashkin and T. I. Kuznetsova, *Kratk. soobshch. fiz.* No. 2, 22 (1984).

Translated by J. G. Adashko